nature astronomy

ARTICLES

https://doi.org/10.1038/s41550-019-0769-0

Magnetic field morphology in interstellar clouds with the velocity gradient technique

Yue Hu[1,2*], Ka Ho Yuen[2], Victor Lazarian[2], Ka Wai Ho[3], Robert A. Benjamin[2], Alex S. Hill[4,5,6], Felix J. Lockman[7], Paul F. Goldsmith[8] and Alex Lazarian[2]

Magnetic fields, while ubiquitous in many astrophysical environments, are challenging to measure observationally. Based on the properties of anisotropy of eddies in magnetized turbulence, the velocity gradient technique is a method synergistic to dust polarimetry that is capable of tracing plane-of-the-sky magnetic fields, measuring the magnetization of interstellar media and estimating the fraction of gravitational collapsing gas in molecular clouds using spectral line observations. Here, we apply this technique to five low-mass star-forming molecular clouds in the Gould Belt and compare the results to the magnetic field orientation obtained from polarized dust emission. We find that the estimates of magnetic field orientations and magnetization for both methods are statistically similar. We estimate the fraction of collapsing gas in the selected clouds. By using the velocity gradient technique, we also present the plane-of-the-sky magnetic field orientation and magnetization of the Smith Cloud, for which dust polarimetry data are unavailable.

Magnetic fields play a crucial role in a variety of important astrophysical processes, from regulating molecular cloud structure formation and evolution[1–3] to constraining star formation in filaments[4–6]. The importance of the magnetic field can be characterized by the ratio of the kinetic energy ~$0.5\rho v_L^2$ to the magnetic energy ~$B^2/8\pi\rho$ in the cloud, where v_L is the turbulent velocity at scale L, ρ is the volume density and B is the magnetic field strength. This quantity is the inverse square of the Alfvén Mach number $(M_A^{-1})^2 = B^2/(4\pi\rho v_L^2)$, a variable used in both the theory of magnetic turbulence and cosmic ray propagation[7].

Owing to advances in dust grain alignment theory[8], the properties of magnetic fields have become more accessible using dust polarization from background starlight or polarized thermal dust emission. For example, the recent Planck survey of polarized dust emission provided us with a comprehensive picture of magnetic field orientations across the full sky[9]. Similarly, dust polarimetric surveys have considerably advanced our knowledge of the magnetic field orientations in molecular clouds[10]. There are, however, challenges when studying the magnetic field through dust polarimetry. For one, dust polarimetry becomes ineffective in the case in which the grains are not aligned. Modern grain alignment theory[11] suggests that grain alignment is driven mainly by radiative torques, but the grains become misaligned in a number of circumstances. For instance, in the absence of sufficiently intense radiation, the orientation of dust grains is random[12]. While in the vicinity of radiation sources dust grains can be aligned with respect to the incident radiation rather than to the ambient magnetic field[12,13]. In addition, it is impossible to separate the contributions of overlapping molecular clouds because dust polarimetry measurements from millimetre, submillimetre or far-infrared emissions sample all the dust along the line of sight. The failure of radiative-torque-driven dust grain alignment mechanisms in high-extinction environments affects further predictions of magnetic field properties based on dust polarimetry measurements, for example using the Davis–Chandrasekhar–Fermi (DCF) technique[14,15].

Apart from dust polarization, there are alternative ways of probing the magnetic field structure. Zeeman measurements allow observers to estimate the signed magnetic field strength along the line of sight and have contributed considerably to our understanding of star formation[16]. However, these measurements require extremely high sensitivity and long integration times. In addition, usually only upper limits of the magnetic field strength are obtained by the Zeeman method. Another tool used to measure the magnetic field strength along the line of sight is Faraday rotation towards polarized radio point sources[17]. Faraday rotation measures the electron density-weighted magnetic field strength along the line of sight and therefore generally does not probe the magnetic field in primarily neutral regions such as molecular clouds. Therefore, there is a demand for alternative methods for probing magnetic fields.

The velocity gradient technique (VGT)[18–21] is a new method capable of tracing the magnetic field orientation in interstellar turbulent media. The technique makes use of the fact that magnetohydrodynamic (MHD) turbulence is anisotropic[22]. It is important that fast turbulent reconnection, the process by which magnetic fields in a conducting fluid change their topology driven by turbulence and independent of fluid resistivity, preferentially induces fluid motions perpendicular to the local magnetic field direction[23]. As a result, gradients of velocities become perpendicular to the local direction of the magnetic field. This phenomenon has been numerically confirmed[24–27] and is the cornerstone of the modern theory of MHD turbulence[7].

The VGT has been numerically tested for a wide range of column densities from diffuse transparent gas[19] to molecular self-absorbing dense gas[28]. It was shown to be able to provide both the orientations of the magnetic field as well as a measure of media magnetization[29]. The VGT has been used to study magnetic field in diffuse H I (refs. [19,20,29,30])

[1]Department of Physics, University of Wisconsin-Madison, Madison, WI, USA. [2]Department of Astronomy, University of Wisconsin-Madison, Madison, WI, USA. [3]Department of Physics, The Chinese University of Hong Kong, Hong Kong, People's Republic of China. [4]Department of Physics and Astronomy, University of British Columbia, Vancouver, British Columbia, Canada. [5]Space Science Institute, Boulder, CO, USA. [6]Dominion Radio Astrophysical Observatory, National Research Council Canada, Penticton, British Columbia, Canada. [7]Green Bank Observatory, Green Bank, WV, USA. [8]Jet Propulsion Laboratory, California Institute of Technology, Pasadena, CA, USA. *e-mail: yue.hu@wisc.edu

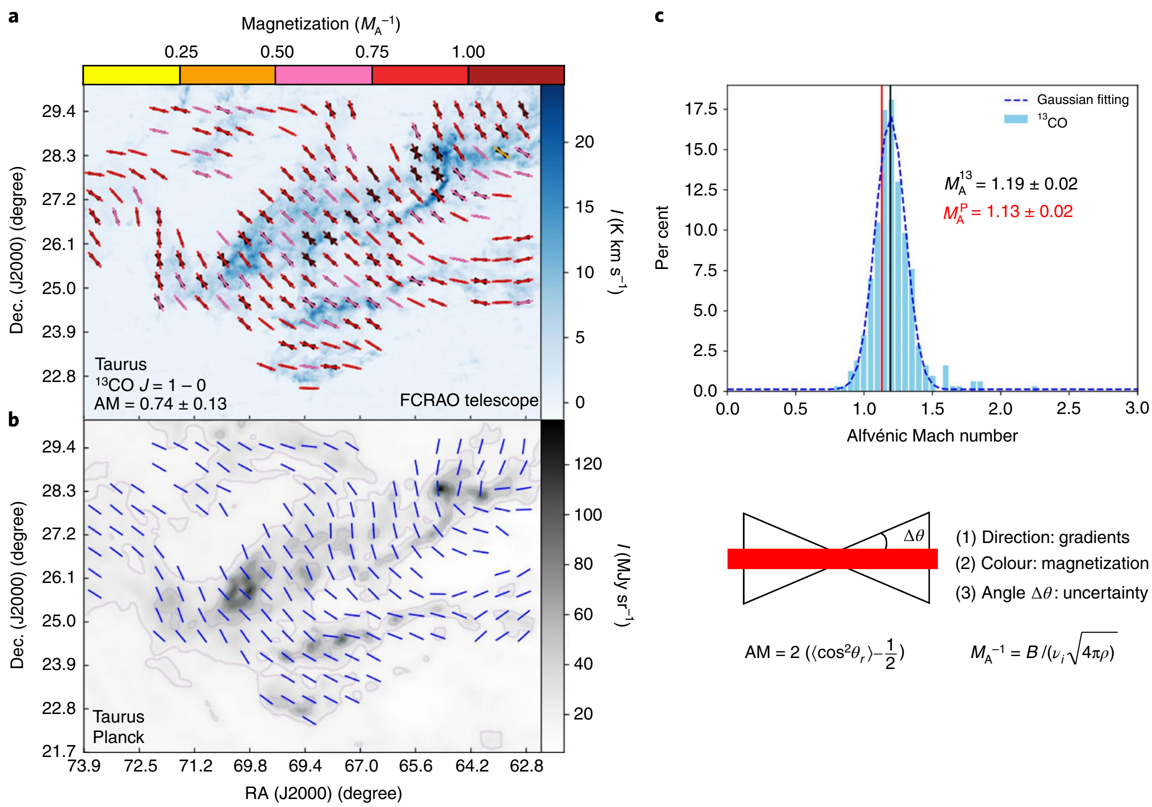

Fig. 1 | The magnetic field morphology of Taurus obtained with the VGT using ^{13}CO and the Planck polarimetry. a, The magnetic field morphology of Taurus obtained with the VGT using ^{13}CO. **b**, The blue line segments indicate the magnetic field morphology of Taurus obtained from the Planck polarimetry. **c**, Histogram of the M_A distribution obtained with the VGT on Taurus. As the VGT provides both the magnetic field orientation and its magnetization, we introduce the bowtie symbol (bottom) that reflects the magnetic field orientation, and magnetization, that is, M_A^{-1} (the different colours of the line segment correspond to different magnetization) and the dispersion of orientations (by variation of the angle θ). M_A^P (red) represents the mean M_A value obtained from the dispersion of polarization orientations, whereas M_A^{13} is the expected value of M_A obtained from the VGT (top) .

and was shown to be complementary to other methods of tracing magnetic field[21]. In this paper we report the application of the VGT to molecular clouds that are known to be turbulent[2,31] and magnetized[16]. While some of the structures in the spectroscopic data may not be due to MHD turbulence, recent studies employing the VGT show a way of identifying these situations and using them to study other important interstellar physics, for example the gravitational collapse of a cloud of interstellar matter[29].

Here, we apply the VGT to five low-mass molecular clouds. The case of massive star formation clouds in which the effects of gravitational collapse are more significant will be investigated elsewhere. This work studies magnetic fields on the scales at which ions and neutrals are well coupled[32] and therefore our expectations based on MHD turbulence theory are applicable. We compare our results with the 353 GHz polarization data from the third Public Data Release (DR3) from the Planck Collaboration in 2018[9]. In addition, to illustrate the abilities of the technique, we present our prediction of magnetic field orientations and magnetization for the Smith Cloud[33], a magnetized high-velocity cloud of atomic hydrogen falling into the Milky Way, for which no optical or infrared polarimetric data are available[34,35].

Results

Morphology of magnetic field traced by the VGT. The molecular clouds to which we apply the VGT are Taurus[36], Perseus A[37], L 1551[38], NGC 1333[39] and Serpens[40]. We use the spectroscopic maps of the molecular tracer ^{13}CO from these molecular clouds to explore the plane-of-the-sky morphology of the magnetic field.

The ^{13}CO data on Taurus and Perseus A were obtained using the 13.7 m Five College Radio Astronomy Observatory telescope, for L1551 the Nobeyama Radio Observatory 45 m telescope, and for NGC 133 and Serpens the Arizona Radio Observatory Heinrich Hertz Submillimeter Telescope. We compare our results to the Planck 353 GHz polarization maps[9], which provide the best representation of the plane-of-the-sky magnetic field orientation of the aforementioned clouds that is available to us. Note that we do not smooth the data from Planck. Instead, we re-sample the Planck data so that the effective resolution matches that of the VGT-predicted magnetic field orientation (see Supplementary Table 1 for the effective resolution). The correspondence of the plane-of-the-sky magnetic field orientations obtained by the VGT and the polarization measurements is quantified using the alignment measure (AM): $\mathrm{AM} = 2\left(\left\langle\cos^2\theta_r\right\rangle - \frac{1}{2}\right)$, where θ_r is the relative angle between the gradients (rotated by 90°) and the orientations of the plane-of-the-sky magnetic field derived from polarization. If the two measures provide identical results, AM = 1.

We adopt the recipe introduced in ref. [20] to trace the plane-of-the-sky orientation of the magnetic field using the gradients of thin velocity channels (VChGs, Ch(x, y)). The selection of thin channel maps (see Methods) increases the weight of velocity contribution to the measured statistics[41]. Owing to the properties of MHD turbulence[42], velocity statistics trace the magnetic field orientation better than density statistics.

Figure 1 shows the VChGs (rotated by 90°) in Taurus, and Fig. 2 shows the results of VChGs for L 1551, Perseus A, NGC 1333 and

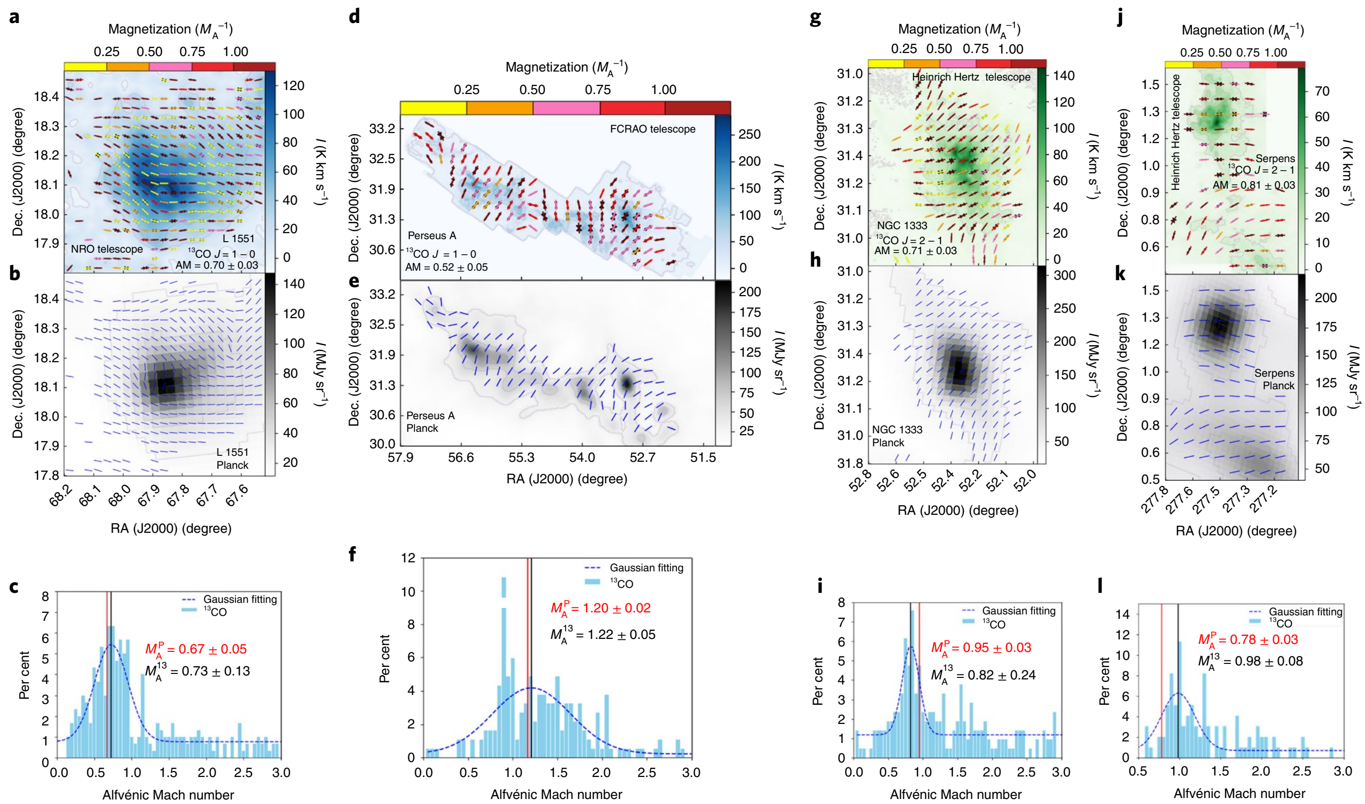

Fig. 2 | The magnetic field morphology of molecular clouds L 1551, Perseus A, NGC 1333 and Serpens obtained with the VGT using ^{13}CO and Planck polarimetry. a,**d**,**g**,**j**, Magnetic field morphology of L 1551 (**a**), Perseus A (**d**), NGC 1333 (**g**), and Serpens (**j**) obtained with the VGT using ^{13}CO (the gradients on NGC 1333 and Serpens are re-rotated). **b**,**e**,**h**,**k**, The blue line segments indicate the magnetic field morphology of L 1551 (**b**), Perseus A (**e**), NGC 1333 (**h**) and Serpens (**k**) obtained from the Planck polarimetry. **c**,**f**,**i**,**l**, Histograms of the M_A distribution obtained with the VGT on L 1551 (**c**), Perseus A (**f**), NGC 1333 (**i**), and Serpens (**l**). We use the same bowtie mark to indicate the orientation of the magnetic field and the magnetization as in Fig. 1. M_A^P represents the mean M_A value obtained from the dispersion of polarization orientations, whereas M_A^{13} is the expected value of M_A obtained from the VGT.

Serpens. For easy visual comparison we overlay the magnetic field orientations predicted by VChGs with those from dust polarization. From Figs. 1 and 2, we see that the magnetic field orientation predicted by VChGs and from dust polarimetry are in good agreement, with a mean statistical deviation of ~4°. More detailed results of the statistical analysis are presented in Table 1 (see the Supplementary Information for an analysis with the histogram of the relative orientation and the alignment distribution map, that is, Supplementary Figs. 3 and 4).

There are differences between the magnetic field orientations traced by the VGT and by the dust polarization observations, but that is expected. Spectroscopic data allow one to separate out different molecular clouds along the line of sight if they have different velocities, but this is not an option for polarized dust radiation. The VGT thus has an advantage for studying magnetic fields, especially for molecular clouds at low galactic latitudes when the foreground and background polarization contributions are important. Other differences include the difference of the accumulation of the signal along the line of sight for gradients and polarization, which is especially important in the case of super-Alfvénic ($M_A > 1$) turbulence[29]. However, the good correlation between the VGT and the polarization measurement of magnetic field orientations shown in Table 1 demonstrates that all these factors are sub-dominant for the clouds studied here. However, regions of gravitational collapse are expected to turn the direction of velocity gradients by 90° with respect to the magnetic fields[43], which we will discuss in the following section.

In ref. [29] it was demonstrated that the magnetization parameterized by the inverse Alfvén Mach number M_A^{-1} can be estimated through the distribution of the velocity gradient orientations within the sub-blocks that are used within our technique (see Supplementary Fig. 5 for details). In general, the distribution of the velocity gradient orientation is Gaussian[19]. More importantly, the width of the distribution is shown to be correlated with the magnetization[29]. In the case of magnetically dominated media ($M_A < 1$), the distribution of velocity gradient orientations is narrower than in turbulence-dominated media. We use the relations between the width of the gradient distribution and magnetization[29] to evaluate the distribution of magnetization in the clouds that we studied. Figures 1 and 2 show the derived distribution of magnetization. For Taurus and Perseus A, we find that the magnetization in high-intensity regions is usually stronger than that in surrounding low-intensity regions. This corresponds to the increasing role of the magnetic field in regions of higher density.

We can use the distribution of polarization orientations over the entire region to obtain the mean magnetization $(M_A^P)^{-1}$. This measure involves the implicit use of the DCF method. The correlation $M_A^P \propto \tan \delta\theta_{pol}$ was numerically proven in ref. [44], where $\delta\theta_{pol}$ is the dispersion of the polarization angle. The mean magnetization can also be obtained by averaging of the local sub-block magnetization values obtained using the VGT. Table 1 illustrates the good correspondence between the two values. The advantage of the VGT compared with the traditional DCF technique is its ability to measure not only the mean magnetization but also a detailed distribution of the magnetization using a self-consistent algorithm[29], which is important for a better understanding of star formation and other key astrophysical processes.

Table 1 | Information about the regions and data used in this work

Cloud region	Taurus	Perseus A	L 1551	Serpens	NGC 1333	Smith Cloud
Emission lines	^{13}CO: $J=1-0$	^{13}CO: $J=1-0$	^{13}CO: $J=1-0$	^{13}CO: $J=2-1$	^{13}CO: $J=2-1$	H I 21 cm
AM	0.74 ± 0.03	0.52 ± 0.05	0.70 ± 0.03	−0.81 ± 0.03	−0.71 ± 0.03	…
M_A	1.19 ± 0.02	1.22 ± 0.05	0.73 ± 0.13	0.98 ± 0.08	0.82 ± 0.24	0.68 ± 0.12
M_A^P	1.13 ± 0.02	1.20 ± 0.02	0.67 ± 0.05	0.78 ± 0.03	0.95 ± 0.03	…
μ	86.12° ± 1.21°	88.72° ± 1.08°	85.10° ± 1.95°	10.06° ± 1.42°	8.08° ± 1.41°	…

All quantities are averages over the regions. AM = 1 indicates perfect alignment between the VGT and the Planck polarization vectors; M_A is the Alfvénic Mach number derived from the VGT; M_A^P is the Alfvénic Mach number derived from the Planck polarization. μ is the expectation value of the relative angle between the un-rotated gradients and the magnetic field derived from the Planck polarization. The uncertainty is given by the standard error of the mean, that is, the standard deviation divided by the square root of the sample size (see Supplementary Information for details).

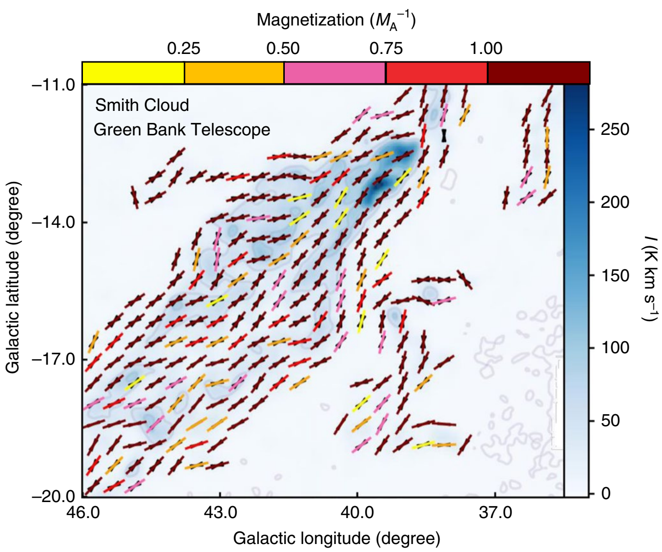

Fig. 3 | The magnetic field morphology and magnetization of the Smith Cloud superimposed on a map of its total H I intensity. We use the same bowtie mark to indicate the orientation of the magnetic field and magnetization as shown in Fig. 1. The colour scale shows the integral of the H I line brightness temperature over velocity.

Neither the polarization measurements nor the VGT trace magnetic fields in molecular clouds perfectly. For the Planck data, the measured signal includes not only the polarization from molecular clouds but also the contributions arising from aligned dust in the interstellar medium in front of and behind the cloud (see Supplementary Information for details on the background removal). For the VGT, the fast MHD modes present in MHD turbulence as well as the effects of gravitational collapse distort the directions of the gradients[20]. In addition, the VGT degrades the resolution of the spectroscopic maps due to the sub-block averaging method. As a trade-off, however, one can get magnetization of the media for every sub-block. Importantly, the degradation of the resolution in the case of the VGT is compensated by the high resolution and good sampling of spectroscopic surveys as well as the abundance of available data. Therefore, the VGT is a valuable method for studying the magnetic field in a large variety of clouds for which no detailed polarization observations are available and in which individual clouds cannot be separated without velocity information.

Gravitational collapse. When turbulence is the dominant mechanism in the dynamics of molecular clouds, that is, before self-gravity comes into play and where there is no distortion due to shocks and outflows, the velocity gradients are perpendicular to the local magnetic field. However, molecular clouds, in general, contain regions of gravitational collapse[45,46]. In the case with gravitational collapse, the infall motions parallel to the magnetic field will gradually dominate the velocity motions due to turbulence. When one measures the gradients of a highly self-gravitating molecular cloud, they follow the direction of the infall, that is, the direction of gradients flips 90° becoming parallel to the magnetic field[43]. This happens because the acceleration of the fluid points towards the core of the collapsing region, thus the direction of the magnetic field and of fluid motions induced by gravitational infall become parallel. To account for this, compensatory re-rotation (that is, rotating the gradients by an additional 90°) must be applied to the gradients[43].

Figure 1 shows the angle uncertainties of VChGs in Taurus, and Fig. 2 shows the uncertainties in Perseus A, L 1551, NGC 1333 and Serpens. We discuss in the Supplementary Information (see Supplementary Fig. 1) that our experimenting with re-rotating the gradient vectors and comparing the resulting gradient map with dust polarimetry indicates that there is no compensatory re-rotation required to obtain good alignment with the magnetic fields derived from Planck on Taurus, L 1551 and Perseus A, but is required for NGC 1333 and Serpens. We thus conclude that the gravitationally collapsing regions constitute only a small fraction of the volume in Taurus, L 1551 and Perseus A. This, however, does not prevent molecular gas in small regions (NGC 1333 and Serpens) from collapsing to form stars[47].

Prediction of magnetic field morphology in the Smith Cloud. We see from Table 1 that the deviation between the average direction of the magnetic fields determined using the VGT and Planck polarimetry is within 5° for Taurus, Perseus A and L 1551, and within 10° for Serpens and NGC 1333, for which the spectroscopic data are noisier. The demonstrated ability of the VGT to trace the magnetic fields encourages us to apply it to interstellar clouds for which no dust polarimetry is available.

The Smith Cloud is a diffuse high-velocity H I cloud with a mean radial velocity of +100 km s^{-1}, which is inconsistent with galactic rotation at its location[33,48,49]. Since the polarization orientation is dominated by the contribution of foreground galactic media along the line of sight, dust polarization measurements are unlikely to reflect the magnetic field structure of the Smith Cloud[34] itself. The advantage of the VGT is that it can provide information on the magnetic field structure of the cloud with limited contamination by the foreground galactic emission. The VGT measures the magnetic fields in the plane of the sky and is complementary to the measurements from previous studies[34,35] that probe the line-of-sight component of the field in ionized gas by measuring the Faraday rotation.

Figure 3 shows the predicted magnetic field orientations for the Smith Cloud using the VGT. The Smith Cloud is a diffuse cloud with no expected gravitational collapse. Therefore, unlike molecular clouds, there should be no need for re-rotations of the velocity gradient orientations. We find that the magnetization of the Smith Cloud is high: $M_A \approx 0.68 \pm 0.12$ (Supplementary Fig. 2). Since in highly magnetized regions the gradients show better alignment with the magnetic field[20], we expect the prediction of the magnetic field morphology to be no less accurate than our results for the molecular clouds discussed previously.

By using the parameters of the Smith Cloud available from the literature[34,49,50], we estimate the strength of the magnetic field $B > 3\,\mu$G in the Smith Cloud. The DCF method is used here, but instead of polarization we use the gradient orientation. The result is consistent with the estimate $B_{||} > 3\,\mu$G by Hill et al.[34] (see Supplementary Information for details).

Methods

The VGT. The pioneering study by Goldreich and Sridhar[22] opened a new era in the theory of MHD turbulence. Fast turbulent reconnection[23], the process by which magnetic fields in a conducting fluid change their topology driven by turbulence and independent of fluid resistivity, is an important part of the modern understanding of the dynamics of the magnetized turbulent eddies that provide the theoretical foundations for the VGT. It has been predicted that magnetic field mixing motions that are perpendicular to the local magnetic field will be favoured[23], since these kinds of motion will induce the least amount of magnetic field back-reaction. As a result, gradients of the fluid motions are expected to be perpendicular to the local magnetic field.

The VGT employs a statistical description of position-position-velocity (PPV) cubes[51]. In ref. [41], the possibility of using the statistics of intensity fluctuations in PPV cubes to study velocity turbulence was explored and subsequent works used PPV cubes to detect the anisotropy of velocity distribution that is induced by the magnetic field[52]. This velocity anisotropy is well reflected in the preferred alignment of the intensity gradients measured in thin channel maps. In addition, the use of thin channels reduces the anonymous crowding effect due to both the overdensity and the opacity, which makes the gradients more aligned with the magnetic field[28]. This is the approach that we use in our present study to trace the magnetic field.

The technique operates as follows: the velocity channel map Ch(x, y) is constructed by creating integrated maps over a narrow velocity range Δv satisfying $\Delta v \le \sqrt{\delta v_R^2}$, where δv_R^2 is the velocity dispersion in a patch size of radius R. We choose the channel width of $\Delta v / \sqrt{\delta v_R^2} \sim 0.5$ so that the velocity contribution in the velocity channel map dominates over the density contribution[20]. We denote the selected velocity channels as thin channels, which can be calculated by integrating over velocity:

$$\mathrm{Ch}(x, y) = \int_{\Delta v^2 \le \delta v_R^2} \mathrm{d}v \; T_\mathrm{R}(x, y, v) \times \mathrm{e}^{-\frac{|v - v_0|^2}{R^2}} \quad (1)$$

where T_R is the radiation temperature of the spectral line in units of kelvin (for H I data T_R is proportional to the density), and v is the line-of-sight velocity. From the velocity channel maps Ch(x, y), the gradient orientation at pixel (x_i, y_j) is defined as:

$$\nabla_{i,j} = \tan^{-1}\left[\frac{\mathrm{Ch}(x_i, y_{j+1}) - \mathrm{Ch}(x_i, y_j)}{\mathrm{Ch}(x_{i+1}, y_j) - \mathrm{Ch}(x_i, y_j)}\right] \quad (2)$$

This creates the pixelized gradient orientation field for the spectroscopic data. When the velocity slice is thin, the channels record the contribution of turbulent velocities[20]. Thus the VChGs method is expected to be applicable to these clouds.

The issue of whether the small-scale structures in neutral hydrogen velocity channel maps are dominated by density or velocity structures has been debated recently[53,54]. However, irrespective of the outcome of these debates, our conclusion that the velocity channel gradients trace magnetic fields well is not affected, especially in the regime of molecular clouds.

Sub-block averaging. The use of sub-block averaging comes from the fact that the orientation of turbulent eddies with respect to the local magnetic field is a statistical concept. In real space the individual gradient vectors are not necessarily required to have any relation to the local magnetic field direction. It has been reported[19] that the velocity gradient orientations in a sub-region—or sub-block—would form a Gaussian distribution in which the peak of the Gaussian fit reflects the 'statistical most probable' magnetic field orientation in this sub–block. As the area of the sampled region increases, the precision of the magnetic field traced through the use of a Gaussian block fit becomes more and more accurate. Subsequently, it was found that the width of the distribution is correlated with the statistical mean magnetization of the sub-region[29]. The use of sub-blocks is a common feature of analyses like ours that use measured gradients in data to connect statistical theories of MHD turbulence to an understanding of gradient orientations in physical space. One should note that sub-block averaging is not just a smoothing method; it provides one with a new statistical measure of the data. A detailed discussion of how white noise affects sub-block averaging versus common smoothing techniques is provided in ref. [19].

Moving window. Another technique developed to improve the performance of the VGT is the moving window (MW) method[20]. The MW method is an attempt to employ sub-block averaging in a continuous rather than a discrete manner. As magnetic fields are continuous, we move the block according to the orientation of the predicted magnetic field to smooth the outlying gradients. When there is an abnormal gradient vector compared with the neighbouring vectors, we rotate the abnormal vector so that a smooth field line is formed. Mathematically, the rotation can be handled by performing smoothing on both the cosines and sines of the raw gradient angle, which is a convolution of an averaging kernel with the raw cosine and sine data.

Previous studies show that there is a limit to how large one can make a MW without the alignment being compromised[20]. The size of the MW chosen here is slightly smaller than the limitation, which not only improves the alignment between the orientations of gradients and dust polarization but also shows visually correct orientations of the gradients. We used 2 pixels as the MW width for Taurus, NGC 1333, L 1551, Serpens and Perseus A. For the Smith Cloud, we chose 1 pixel as the MW width.

Observational data. *Taurus.* The Taurus Molecular Cloud[36] region was measured in the $J = 1-0$ transition of ^{13}CO using the 13.7 m millimeter-wave telescope of the Five College Radio Astronomy Observatory (FCRAO). The data cover approximately 100 deg^2 of the sky (11.5° in RA by 8.5° in dec.) corresponding to a region 28 pc × 21 pc at a distance of 140 pc. The high angular resolution of 47" allows one to examine in detail the relatively fine structures along with the large-scale distribution of the molecular material and the magnetic field. The root mean square (r.m.s.) 1σ noise level is 0.18 K for ^{13}CO in an individual pixel.

Serpens and NGC 1333. The Serpens cloud[40], which extends across a 50′ × 60′ region corresponding to 5.3 pc × 7.6 pc at a distance of 415 pc, is a low-mass star-forming cloud in the Gould Belt, while NGC 1333[39] is a 50′ × 60′ section of the Perseus Molecular Cloud (3.4 pc × 4.1 pc at a distance of 235 pc). The ^{13}CO $J = 2-1$ emission data (220.4 GHz) on both regions were obtained by the Arizona Radio Observatory Heinrich Hertz Submillimeter Telescope. The angular resolution is 38″ (0.04 pc) and velocity resolution is 0.3 km s^{-1}. The r.m.s. 1σ noise level is 0.11 K for both data in an individual pixel.

Perseus A. The Perseus molecular cloud[37] is a nearby giant molecular cloud in the constellation of Perseus. The ^{13}CO $J = 1-0$ emission data of Perseus A were taken from the COMPLETE Survey using the FCRAO telescope at an angular resolution of approximately 46″. The r.m.s. 1σ noise level is 0.15 K in an individual pixel.

L 1551. L 1551[38] is relatively isolated in the Taurus Molecular Cloud. Observations of the $J = 1-0$ transition of ^{13}CO were made using the Nobeyama Radio Observatory (NRO) 45 m telescope equipped with the 25-BEam Array Receiver System (BEARS) receiver. The data cover ~40′ × 40′ with a resolution of ~30″, yielding maps with the highest spatial resolution. The r.m.s. 1σ noise level is 0.94 K in an individual pixel.

Smith Cloud. The Smith Cloud[34] is one of the best high-velocity clouds for tracing the interaction between the galactic halo and interstellar medium. It covers a 10.5° × 9° region at a distance of 12.4 kpc. The H I data used here were obtained using the Rebert C. Byrd Green Bank Telescope. The spectra cover 700 km s^{-1} around zero local standard of rest velocity at a velocity resolution of 0.65 km s^{-1} and the angular resolution is 9.1′, while the typical r.m.s. 1σ noise level is 90 mK in a 0.65 km s^{-1} channel.

Planck Mission. Planck (http://www.esa.int/Planck) is a project of the European Space Agency (ESA), with contributions from NASA (USA) and telescope reflectors provided by a collaboration between the ESA and a scientific consortium led and funded by Denmark. The Planck data we used here is Planck HFI Products for Public Data Release 3 2018[9]. The data are from the study of the polarized thermal emission from galactic dust, using the High Frequency Instrument at 353 GHz with angular resolution 5′.

Data availability

The data that support the plots within this paper and other findings of this study are available from the corresponding author and other co-authors upon reasonable request.

Code availability

The code for the VGT algorithm is available at https://github.com/wisYue/Survey.git.

Received: 15 October 2018; Accepted: 29 March 2019;
Published online: 10 June 2019

References

1. Planck Collaboration Planck intermediate results. XXXV. Probing the role of the magnetic field in the formation of structure in molecular clouds. *Astron. Astrophys.* **586**, A138 (2016).

2. Larson, R. B. Turbulence and star formation in molecular clouds. *Mon. Not. R. Astron. Soc.* **194**, 809–826 (1981).
3. McKee, C. F. & Tan, J. C. The formation of massive stars from turbulent cores. *Astrophys. J.* **585**, 850–871 (2003).
4. Seifried, D. & Walch, S. The impact of turbulence and magnetic field orientation on star-forming filaments. *Mon. Not. R. Astron. Soc.* **452**, 2410–2422 (2015).
5. Bromm, V., Coppi, P. S. & Larson, R. B. Forming the first stars in the Universe: the fragmentation of primordial gas. *Astrophys. J. Lett.* **527**, L5–L8 (1999).
6. Hill, T. et al. Filaments and ridges in Vela c revealed by Herschel: from low-mass to high-mass star-forming sites. *Astron. Astrophys.* **533**, A94 (2011).
7. Brandenburg, A. & Lazarian, A. Astrophysical hydromagnetic turbulence. *Space Sci. Rev.* **178**, 163–200 (2013).
8. Andersson, B.-G., Lazarian, A. & Vaillancourt, J. E. Interstellar dust grain alignment. *Annu. Rev. Astron. Astrophys.* **53**, 501–539 (2015).
9. Planck Collaboration Planck 2018 results. III. High Frequency Instrument data processing and frequency maps. Preprint at https://arxiv.org/abs/1807.06207 (2018).
10. Li, H.-B. et al. Self-similar fragmentation regulated by magnetic fields in a region forming massive stars. *Nature* **520**, 518–521 (2015).
11. Lazarian, A. Magnetic fields via polarimetry: progress of grain alignment theory. *J. Quant. Spectrosc. Radiat. Transf.* **79**, 881 (2003).
12. Lazarian, A. & Hoang, T. Subsonic mechanical alignment of irregular grains. *Astrophys. J.* **669**, L77–L80 (2007).
13. Hoang, T., Cho, J. & Lazarian, A. Alignment of irregular grains by mechanical torques. *Astrophys. J.* **852**, 129 (2018).
14. Davis, L. The strength of interstellar magnetic fields. *Phys. Rev.* **81**, 890–891 (1951).
15. Chandrasekhar, S. & Fermi, E. Magnetic fields in spiral arms. *Astrophys. J.* **118**, 113 (1953).
16. Crutcher, R. M., Wandelt, B., Heiles, C., Falgarone, E. & Troland, T. H. Magnetic fields in interstellar clouds from Zeeman observations: inference of total field strengths by Bayesian analysis. *Astrophys. J.* **725**, 466–479 (2010).
17. Taylor, A. R., Stil, J. M. & Sunstrum, C. A rotation measure image of the sky. *Astrophys. J.* **702**, 1230–1236 (2009).
18. González-Casanova, D. F. & Lazarian, A. Velocity gradients as a tracer for magnetic fields. *Astrophys. J.* **835**, 41 (2017).
19. Yuen, K. H. & Lazarian, A. Tracing interstellar magnetic field using velocity gradient technique: application to atomic hydrogen data. *Astrophys. J.* **837**, L24 (2017).
20. Lazarian, A. & Yuen, K. H. Tracing magnetic fields with spectroscopic channel maps. *Astrophys. J.* **853**, 96 (2018).
21. Yuen, K. H. et al. Statistical tracing of magnetic fields: comparing and improving the techniques. *Astrophys. J.* **865**, 54 (2018).
22. Goldreich, P. & Sridhar, S. Toward a theory of interstellar turbulence. 2: strong Alfvénic turbulence. *Astrophys. J.* **438**, 763–775 (1995).
23. Lazarian, A. & Vishniac, E. T. Reconnection in a weakly stochastic field. *Astrophys. J.* **517**, 700–718 (1999).
24. Cho, J. & Vishniac, E. T. The anisotropy of magnetohydrodynamic Alfvénic turbulence. *Astrophys. J.* **539**, 273–282 (2000).
25. Maron, J. & Goldreich, P. Simulations of incompressible magnetohydrodynamic turbulence. *Astrophys. J.* **554**, 1175–1196 (2001).
26. Beresnyak, A. & Lazarian, A. Scaling laws and diffuse locality of balanced and imbalanced magnetohydrodynamic turbulence. *Astrophys. J. Lett.* **722**, L110–L113 (2010).
27. Beresnyak, A. & Lazarian, A. in *Magnetic Fields in Diffuse Media* (eds Lazarian, A., de Gouveia Dal Pino, E. M. & Melioli, C.) 163–226 (Springer, 2015).
28. Hsieh, C.-h. et al. Tracing magnetic field morphology using the velocity gradient technique in the presence of CO self-absorption. *Astrophys. J.* **873**, 16 (2019).
29. Lazarian, A. et al. Distribution of velocity gradient orientations: mapping magnetization with the velocity gradient technique. *Astrophys. J.* **865**, 46 (2018).
30. Hu, Y., Yuen, K. H. & Lazarian, A. Improving the accuracy of magnetic field tracing by velocity gradients: principal component analysis. *Mon. Not. R. Astron. Soc.* **480**, 1333–1339 (2018).
31. Ostriker, E. C., Stone, J. M. & Gammie, C. F. Density, velocity, and magnetic field structure in turbulent molecular cloud models. *Astrophys. J.* **546**, 980–1005 (2001).
32. Xu, S. & Lazarian, A. Magnetohydrodynamic turbulence and turbulent dynamo in partially ionized plasma. *New J. Phys.* **19**, 065005 (2017).
33. Smith, G. P. A peculiar feature at $l^{II}=40°.5$, $b^{II}=-15°.0$. *Bull. Astron. Institutes Netherlands* **17**, 203 (1963).
34. Hill, A. S., Mao, S. A., Benjamin, R. A., Lockman, F. J. & McClure-Griffiths, N. M. Magnetized gas in the Smith High Velocity Cloud. *Astrophys. J.* **777**, 55 (2013).
35. Betti, S. K. et al. Constraining the magnetic field of the Smith High-Velocity Cloud using Faraday rotation. *Astrophys. J.* **871**, 215 (2019).
36. Goldsmith, P. F. et al. Large-scale structure of the molecular gas in Taurus revealed by high linear dynamic range spectral line mapping. *Astrophys. J.* **680**, 428–445 (2008).
37. Ridge, N. A. et al. The complete survey of star-forming regions: phase I data. *Astrophys. J.* **131**, 2921–2933 (2006).
38. Lin, S.-J. et al. The intrinsic abundance ratio and X-factor of CO isotopologues in L 1551 shielded from FUV photodissociation. *Astrophys. J.* **826**, 193 (2016).
39. Bieging, J. H., Revelle, M. & Peters, W. L. The Arizona Radio Observatory CO mapping survey of galactic molecular clouds. IV. The NGC 1333 cloud in Perseus in CO $J=2-1$ and ^{13}CO $J=2-1$. *Astrophys. J. Suppl. Ser.* **214**, 7 (2014).
40. Burleigh, K. J., Bieging, J. H., Chromey, A., Kulesa, C. & Peters, W. L. The Arizona Radio Observatory CO mapping survey of galactic molecular clouds. III. The Serpens cloud in CO $J=2-1$ and ^{13}CO $J=2-1$ emission. *Astrophys. J. Suppl. Ser.* **209**, 39 (2013).
41. Lazarian, A. & Pogosyan, D. Velocity modification of H I power spectrum. *Astrophys. J.* **537**, 720–748 (2000).
42. Cho, J. & Lazarian, A. Compressible magnetohydrodynamic turbulence: mode coupling, scaling relations, anisotropy, viscosity-damped regime and astrophysical implications. *Mon. Not. R. Astron. Soc.* **345**, 325–339 (2003).
43. Yuen, K. H. & Lazarian, A. Tracing interstellar magnetic field using the velocity gradient technique in shock and self-gravitating media. Preprint at https://arXiv.org/abs/1703.03026 (2017).
44. Falceta-Gonçalves, D., Lazarian, A. & Kowal, G. Studies of regular and random magnetic fields in the ISM: statistics of polarization vectors and the Chandrasekhar-Fermi technique. *Astrophys. J.* **679**, 537 (2008).
45. Zhang, Q., Wang, K., Lu, X. & Jiménez-Serra, I. Fragmentation of molecular clumps and formation of a protocluster. *Astrophys. J.* **804**, 141 (2015).
46. Ballesteros-Paredes, J., Klessen, R. S., Mac Low, M.-M. & Vazquez-Semadeni, E. in *Protostars and Planets V* (eds Reipurth, B., Jewitt, D. & Keil, K.) 63–80 (Univ. Arizona Press, 2007).
47. Sugitani, K. et al. Near-infrared-imaging polarimetry toward Serpens South: revealing the importance of the magnetic field. *Astrophys. J.* **734**, 63 (2011).
48. Bland-Hawthorn, J. et al. The Smith cloud: H I associated with the Sgr dwarf? *Mon. Not. R. Astron. Soc.* **299**, 611–624 (1998).
49. Lockman, F. J., Benjamin, R. A., Heroux, A. J. & Langston, G. I. The Smith Cloud: a high-velocity cloud colliding with the Milky Way. *Astrophys. J. Lett.* **679**, L21–L24 (2008).
50. Wakker, B. P. et al. Distances to galactic high-velocity clouds. I. Cohen Stream, Complex GCP, cloud g1. *Astrophys. J.* **672**, 298–319 (2008).
51. Lazarian, A. & Pogosyan, D. Studying velocity turbulence from Doppler-broadened absorption lines: statistics of optical depth fluctuations. *Astrophys. J.* **686**, 350–362 (2008).
52. Lazarian, A., Pogosyan, D. & Esquivel, A. Quest for H I turbulence statistics: new techniques. In *Seeing Through the Dust: The Detection of H I and the Exploration of the ISM in Galaxies, Astronomical Society of the Pacific Conference Series* (eds Taylor, A. R., Landecker, T. L. & Willis, A. G.) **276**, 182 (2002).
53. Clark, S. E., Peek, J. E. G. & Miville-Deschênes, M. A. The physical nature of neutral hydrogen intensity structure. Preprint at https://arXiv.org/abs/1902.01409 (2019).
54. Yuen, K. H., Hu, Y., Lazarian, A. & Pogosyan, D. Comment on Clark et al. (2019) "The physical nature of neutral hydrogen intensity structure". Preprint at https://arXiv.org/abs/1904.03173 (2019).

Acknowledgements

A.L. acknowledges the support of National Science Foundation (NSF) grants AST 1715754 and 1816234, and NASA grant NNX14AJ53G. The research of P.F.G. was carried out at the Jet Propulsion Laboratory, which is operated for NASA by the California Institute of Technology. We acknowledge M. Heyer for a number of valuable suggestions in improving our paper. We acknowledge the COordinated Molecular Probe Line Extinction Thermal Emission Survey of Star Forming Regions (COMPLETE) for providing a range of data for the Perseus region and the Arizona Radio Observatory for providing the data of the Serpens region and NGC 1333. The Green Bank Observatory is a facility of the NSF operated under a cooperative agreement by Associated Universities, Inc. This work is based on observations obtained with Planck (http://www.esa.int/Planck), an ESA science mission with instruments and contributions directly funded by the ESA Member States, NASA and Canada.

Author contributions

All authors discussed the results, commented on the manuscript and contributed to the writing of the manuscript. Y.H., K.H.Y. and A.L. conceived the project, Y.H., K.H.Y. and K.W.H. performed calculations, while Y.H., K.H.Y., V.L. and A.L. analysed the results and wrote the original manuscript. R.A.B. provided suggestions on how the VGT technique

might be applied to the Smith Cloud. The data on the Taurus cloud were provided by P.F.G. and data on the Smith Cloud were provided by A.S.H. and F.J.L.

Competing interests

The authors declare no competing interests.

Additional information

Supplementary information is available for this paper at https://doi.org/10.1038/s41550-019-0769-0.

Reprints and permissions information is available at www.nature.com/reprints.

Correspondence and requests for materials should be addressed to Y.H.

Journal peer review information: *Nature Astronomy* thanks Andrea Bracco, Kate Pattle and Thomas H. Troland for their contribution to the peer review of this work.

Publisher's note: Springer Nature remains neutral with regard to jurisdictional claims in published maps and institutional affiliations.